Studies of Structure-Activity Relations of Complement Inhibitor Compstatin[1]

Athena M. Soulika,* Dimitrios Morikis,† Maria-Rosa Sarrias,* Melinda Roy,‡ Lynn A. Spruce,* Arvind Sahu,§ John D. Lambris[2]*

Compstatin, a 13-mer cyclic peptide, is a novel and promising inhibitor of the activation of the complement system. In our search for a more active analog and better understanding of structure-functions relations, we designed a phage-displayed random peptide library based on previous knowledge of structure activity relations, in which seven amino acids deemed necessary for structure and activity were kept fixed while the remaining six were optimized. Screening of this library against C3 identified four binding clones. Synthetic peptides corresponding to these clones revealed one analog, called acetylated Ile[1]Leu/His[9]Trp/Thr[13]Gly triple replacement analog of compstatin corresponding to clone 640 (Ac-I1L/H9W/T13G), which was more active than compstatin. This newly identified peptide had 4-fold higher activity when compared with the originally isolated form of compstatin and 1.6-fold higher activity when compared with acetylated compstatin (Ac-compstatin). The structures of Ac-I1L/H9W/T13G and Ac-compstatin were studied by nuclear magnetic resonance, compared with the structure of compstatin, and found to be very similar. The binding of Ac-I1L/H9W/T13G and the equally active acetylated analog with His[9]Ala replacement (Ac-H9A) to C3 was evaluated by surface plasmon resonance, which suggested similarity in their binding mechanism but difference when compared with Ac-compstatin. Compensatory effects of flexibility outside the β-turn and tryptophan ring stacking may be responsible for the measured activity increase in Ac-I1L/H9W/T13G and acetylated analog with His[9]Ala replacement and the variability in binding mechanism compared with Ac-compstatin. These data demonstrate that tryptophan is a key amino acid for activity. Finally, the significance of the N-terminal acetylation was examined and it was found that the hydrophobic cluster at the linked termini of compstatin is essential for binding to C3 and for activity. ***The Journal of Immunology*****, 2003, 170: 1881–1890.**

Compstatin, a 13-mer peptide (Ile[1]-Cys[2]-Val[3]-Val[4]-Gln[5]-Asp[6]-Trp[7]-Gly[8]-His[9]-His[10]-Arg[11]-Cys[12]-Thr[13]-NH_2) cyclized through a disulfide bridge, is an inhibitor of the activation of the complement system and was initially isolated from a phage-displayed random peptide library screened against C3b (1). Compstatin binds to native C3 and inhibits its cleavage by the C3 convertases of the classical, lectin, and alternative pathways in a manner that is not due to sterical hindrance (1).

Compstatin has been successfully tested in a model of hyperacute rejection in discordant kidney xenotransplantation (2) and in models of extracorporeal circulation (3). In the xenotransplantation model, compstatin significantly prolonged the survival of the kidneys (2), whereas in the models of extracorporeal circulation it inhibited the generation of C3a and sC5b-9 and activation of polymorphonuclear leukocytes (3). The efficacy of compstatin has also been evaluated in an in vivo model of complement activation in baboons (4). In this model, compstatin completely inhibited complement activation and exhibited no toxic effects in all doses tested, suggesting that it may be both a safe and effective complement inhibitor.

All of these studies have rendered compstatin one of the most interesting inhibitors of the activation of complement system. Moreover, its small size adds further value to this inhibitor in that it can serve as a prototype for an orally administered drug (5–7).

The interaction between C3 and compstatin has been the focus of our attention. In recent studies in our laboratory, we have used surface plasmon resonance technology to analyze the nature of this interaction (8). These studies have shown that, although the binding of compstatin to C3b and C3c is a simple interaction that follows the 1:1 Langmuir model, this is not the case for the binding of compstatin to C3 and $C3H_2O$, where the interaction seems to be more complex, consisting of more than one phase. In addition, the same studies have shown that compstatin is able to bind to C3 and its fragments C3b and C3c only when it is immobilized on the sensor chip via its C terminus, underlining the importance of the accessibility of the peptide N terminus. Participation of the N terminus in binding was further supported by the fact that upon *N*-acetylating, the inhibitory activity of compstatin was increased by 3-fold (8, 9). We have previously determined the structure of a major conformer of compstatin in solution using nuclear magnetic resonance (NMR)[3] spectroscopy (10, 11). Compstatin forms a type I β-turn in the region Gln[5]-Asp[6]-Trp[7]-Gly[8]. In addition, compstatin possesses a hydrophobic cluster at the opposite side of the

*Department of Pathology and Laboratory Medicine, School of Medicine, University of Pennsylvania, Philadelphia, PA 19104; †Department of Chemical and Environmental Engineering, University of California, Riverside, CA 92521; ‡Department of Chemistry and Biochemistry, University of California at San Diego, La Jolla, CA 92093; and §National Center for Cell Science, Pune University Campus, Ganeshkhind, Pune, India

Received for publication March 28, 2003. Accepted for publication June 4, 2003.

The costs of publication of this article were defrayed in part by the payment of page charges. This article must therefore be hereby marked *advertisement* in accordance with 18 U.S.C. Section 1734 solely to indicate this fact.

[1] This work was supported by National Institutes of Health Grants GM62134 and AI30040 and by Grant-in-Aid Award 0255757Y from the American Heart Association. A.S. is a Wellcome Trust Overseas Senior Research Fellow in Biomedical Science in India.

[2] Address correspondence and reprint requests to Dr. John D. Lambris, Protein Chemistry Laboratory, 401 Stellar-Chance Labs, 422 Curie Boulevard, School of Medicine, University of Pennsylvania, Philadelphia, PA 19104. E-mail address: lambris@mail.med.upenn.edu

[3] Abbreviations used in this paper: NMR, nuclear magnetic resonance; Ac-I1L/H9W/T13G, acetylated Ile[1]Leu/His[9]Trp/Thr[13]Gly triple replacement analog of compstatin corresponding to clone 640; Ac-compstatin, acetylated compstatin; 2D, two-dimensional; Ac-H9A, acetylated analog with His[9]Ala replacement; TFA, trifluoroacetic acid; Er, rabbit erythrocyte; NHS, normal human serum; GVB, gelatin veronal buffer; TOCSY, total correlation spectroscopy; NOESY, nuclear Overhauser effect spectroscopy; compstatin-phage, phage-bound compstatin.

0022-1767/03/$02.00

β-turn involving residues at the linked termini Ile^1-Cys^2-Val^3-Val^4-Cys^{12}-Thr^{13}. An Ala scan indicated that the amino acids Cys^2, Val^3, and Cys^{12} of the hydrophobic cluster and the amino acids of the β-turn are essential for the activity of compstatin in vitro (8, 10). Studies of the inhibitory activity of a linear compstatin analog, where Cys^2 and Cys^{12} were reduced and alkylated, or analogs with reduced length between the two cysteines resulted in inactive peptides (8, 10). Additional NMR and inhibitory activity studies of seven compstatin analogs designed to enhance or disrupt structure and/or function were used as an aid to determine which structural elements are important for the structural stability and inhibitory activity of compstatin (12). Based on these studies, we proposed that the four residues of the β-turn and the disulfide bridge between Cys^2-Cys^{12} are essential for both structural stability and inhibitory activity of compstatin. We also proposed that three of six residues of the hydrophobic cluster are essential for inhibitory activity of compstatin, with residues Cys^2, Cys^{12}, and Val^3 being indispensable for inhibition (8, 10, 12).

The aim of the present study is to understand the structure-function relations of compstatin and to optimize the amino acids outside the disulfide bridge, Val^3, and β-turn that contribute to the inhibitory activity of compstatin. Based on the above structure-activity correlations, we designed a random phage-displayed peptide library of the type Xaa^1-Cys^2-Val^3-Xaa^4-Gln^5-Asp^6-Trp^7-Gly^8-Xaa^9-Xaa^{10}-Xaa^{11}-Cys^{12}-Xaa^{13}, in which the six amino acids marked with Xaa were randomized and the remaining seven amino acids were kept constant. This library was screened against C3, and the clones that bound C3 were further analyzed and characterized. This analysis led to the identification of an acetylated synthetic peptide analog of compstatin named acetylated Ile^{1}Leu/His^{9}Trp/Thr^{13}Gly triple replacement analog of compstatin corresponding to clone 640 (Ac-I1L/H9W/T13G) that is 1.6 times more active than acetylated compstatin (Ac-compstatin) when tested in a complement-mediated hemolytic assay. The Ac-I1L/H9W/T13G peptide is four times more active than the originally isolated form of compstatin (1, 8). The molar ratio of C3 to peptide at which the new analog inhibited 50% of hemolytic activity was 1:6. The structure of Ac-I1L/H9W/T13G was studied by two-dimensional (2D) NMR and was compared for consistency with the structure of parent peptides compstatin and Ac-compstatin. The spectra of Ac-compstatin will be presented here for first time. To gain insight into the binding mechanism, the binding of Ac-I1L/H9W/T13G to C3 was examined using surface plasmon resonance and was compared with the binding of Ac-compstatin and acetylated analog with His^{9}Ala replacement (Ac-H9A) to C3. Ac-H9A is an equally active compstatin analog to Ac-I1L/H9W/T13G, and both of them are the most active compstatin analogs found to date. Finally, the role played by the charge at the N terminus in the binding of compstatin to C3 was investigated.

Materials and Methods

Purified proteins

Human C3 was purified from serum as previously described (13). Native C3 was separated from C3 (H_2O) using a Mono S column (Pharmacia, Piscataway, NJ) as described elsewhere (14).

Construction of the phage-displayed random peptide library

The construction of the phage peptide library was done as described elsewhere (15), with the difference that the library was plated without amplification. Each plaque formed was amplified in *Escherichia coli* DH5*a*F′ (Life Technologies, Rockville, MD) as described (16), and the supernatants were tested for binding to C3. The combinatorial gene sequences displayed at the N terminus of the M13 pIII gene were of the form NNS TGC GTG NNS CAG GAC TGG GGC $(NNS)_3$ TGC NNS, where N represents all four nucleotides (A, C, G, and T) in an equal molar ratio, and S represents an equal molar ratio of C, G, and T. The encoded amino acid scheme was Xaa^1-Cys^2-Val^3-Xaa^4-Gln^5-Asp^6-Trp^7-Gly^8-Xaa^9-Xaa^{10}-Xaa^{11}-Cys^{12}-Xaa^{13}, where Xaa represents any natural amino acid.

Selection of positive clones

Microtiter wells (Nunc, Naperville, IL) were coated with 50 μl of 10 μg/ml C3 in PBS for 2 h. The wells were then blocked with 1% nonfat milk in PBS for 1 h, and dilutions of phages' supernatants (1:4 in blocking solution) were added. In parallel, equal titers of phage were added to microtiter wells coated with blocking solution and served as negative controls. The wells were incubated for 1 h and then were washed twice with 200 μl of PBS containing 0.05% Tween 20 (PBS-T). Fifty microliters of 1/1000 anti-M13 mAb conjugated to HRP (Pharmacia) were added to each well and incubated for 40 min. After three washes with 200 μl of PBS-T, the binding was detected with addition of the HRP substrate (0.05% ABTS in 0.1 M sodium citrate (pH 4.2)). The plates were read at 405 nm. All steps were performed at ambient temperature.

Phage sequencing

Individual plaques (clones) were amplified in *E. coli*, and the dsDNAwas purified (Wizard Plus Miniprep DNA purification system; Promega, Madison, WI) and sequenced by automated cycle sequencing (ABI 377 or 373A stretch sequencers; Applied Biosystems, Foster City, CA) using *Taq* FS dye terminator (Applied Biosystems) or dye primer chemistry. An oligonucleotide primer with the sequence 5′-AGC GTA ACG ATC TAA A-3′ was used to determine the nucleotide sequence of the unique region of the M13 phage.

Peptide synthesis purification and characterization

Compstatin and its analogs were synthesized in an Applied Biosystems peptide synthesizer (model 431A) using F-moc amide resin (4-(2′,4′-dimethoxyphenyl-F-moc-aminomethyl)-phenoxy resin). The side chain protecting groups were Cys (Acm), Asp (otBu), Arg (Pmc), Thr (tBu), Gln (Trt), Trp (Boc), and His (Trt). All peptides were cleaved from the resin by incubation for 3 h at 22°C with a solvent mixture containing 5% phenol, 5% water, 2.5% triisoproposilane, and 87.5% trifluoroacetic acid (TFA). The reaction mixture was filtered though a fritted funnel, precipitated with cold ether, dissolved in 50% acetonitrile containing 0.1% TFA, and lyophilized. The crude peptides obtained after cleavage were dissolved in 10% acetonitrile containing 0.1% TFA and were purified using a C-18 reversed-phase column (Waters, Milford, MA). Cyclization of the cyclic peptides was performed on resin using 1.5 M excess of thalium(III) trifluoracetate in dimethylformamide. *N*-acetylation of all peptides was achieved by treating them with a solution of 0.5 M acetic anhydride, 0.125 M diisopropylethylamine, and 0.015 M 1-hydroxy-benzotrazide for 5 min (Applied Biosystems). The purity and identity of the peptides were critically monitored by analytical chromatography on a reversed-phase C-18 column and by laser desorption mass spectrometry (17). Formation of disulfide bond in each peptide was confirmed by mass spectrometry using a mass shift assay that involves reactions of thiols with *p*-hydroxy mercuric benzoic acid (18).

Inhibition of compstatin-phage binding to C3 by compstatin and its analogs

Microtiter wells (Nunc) were coated with 50 μl of 10 μg/ml C3 in PBS for 2 h. The wells were then blocked with 1% nonfat milk in PBS for 1 h, and 25 μl of different concentrations of Ac-compstatin (peptide) and its analogs were added and incubated for 20 min. Twenty-five microliters of compstatin-phage solution (5×10^7 PFU) were added directly to each well and they were further incubated for 30 min. After two washes with 200 μl of PBS-T, 50 μl of 1/1000 diluted anti-M13 mAb conjugated to HRP was added to each well. After 40-min incubation, the wells were washed three times with 200 μl of PBS-T, and the binding was detected by addition of the HRP substrate (0.05% ABTS in 0.1 M sodium citrate (pH 4.2)). The plates were read at 405 nm. The assay was performed at room temperature. The percentage of binding obtained was normalized by considering 100% binding to be equal to the binding occurring in the absence of the peptide. The concentration of the peptide causing 50% inhibition of the compstatin-phage binding to C3 was taken as IC_{50}.

Complement-mediated hemolytic assay

Inhibition of complement activity by compstatin and its analogs was evaluated by measuring their effect on the activation of the alternative pathway of complement. Inhibition of the complement alternative pathway was determined by measuring the lysis of rabbit erythrocytes (Er) by normal human serum (NHS) as previously described (19). Various concentrations of

peptides were mixed with 8 μl of NHS, 5 μl of 0.1 M Mg^{2+} EGTA, and 10 μl of Er (10^9 cells/ml), and the final volume was adjusted to 100 μl with gelatin veronal buffer (GVB). The reaction mixture was incubated at 37°C and stopped by adding 200 μl of GVB with 10 mM EDTA. After centrifugation, the lysis of Er was determined by reading absorbance at 405 nm. The percentage of lysis obtained was normalized by considering 100% lysis to be equal to the lysis occurring in the absence of the peptide. The concentration of the peptide causing 50% inhibition of hemolytic activity was taken as IC_{50}. All of the peptides tested were blocked by acetyl and NH_2 groups at the N and C termini, respectively.

NMR studies of Ac-I1L/H9W/T13G and Ac-compstatin

The NMR samples were prepared in 90% H_2O-10% D_2O buffer containing 50 mM potassium phosphate and 100 mM potassium chloride. The pH of the samples was ~6.5 and their concentration was ~5 mM. In the case of the Ac-I1L/H9W/T3G sample, some precipitation appeared in the NMR tube.

NMR spectra were collected using a DMX 500-MHz spectrometer (Bruker, Billerica, MA) at 5°C. Two-dimensional total correlation spectroscopy (TOCSY) and nuclear Overhauser effect spectroscopy (NOESY) spectra were collected using standard pulse sequences (20) and references therein and the 3-9-19 pulse sequence with gradients for water suppression (21). The TOCSY mixing time was 60 ms, and the NOE mixing time was 150 ms and 500 ms for Ac-compstatin and Ac- I1L/H9W/T3G analog, respectively.

Spectral processing was performed using matNMR, which is a toolbox for processing NMR/EPR data (http://www.nmr.ethz.ch/matnmr; written by J. van Beek) under MATLAB (The Mathworks, Natick, MA). Apodization was performed using Gaussian or cosine squared window functions. The solvent was deconvoluted from the spectra using the time domain convolution method of Marion et al. (22) with a sine bell function.

Surface plasmon resonance studies

The binding of Ac-compstatin and its analogs to native C3 was examined on surface plasmon resonance-based biosensors Biacore-X and Biacore 3000 (Biacore, Piscataway, NJ) using streptavidin chips (sensor chip SA; Biacore). The binding experiments were performed at room temperature and the running buffer used was PBS supplemented with 0.05% Tween 20 to reduce nonspecific binding. We synthesized biotinylated analogs of the peptides that were immobilized on the sensor chips in an oriented fashion. This assured the homogeneity of the surface. In the Biacore-X model, the control peptide (the linear analog of compstatin Ac-IAVVQDWGHHRAT AGHMANLTSHASAK-biotin) was immobilized on flow cell-1, and one of the target peptides (Ac-compstatin, Ac-ICVVQDWGHHRCTAGH MANLTSHASAK-biotin; Ac-H9A, Ac-ICVVQDWGAHRCTAGHMAN LTSHASAK-biotin; or Ac-I1L/H9W/T13G, Ac-LCVVQDWGWHRC GAGHMANLTSHASAK-biotin) was immobilized on flow cell-2. The C terminus tag was designed based on the sequence of the original compstatin clone (1). When Biacore-3000 was used, the linear peptide was immobilized on flow cell-1, and Ac-compstatin, Ac-H9A, and Ac-I1L/H9W/T13G were immobilized on flow cells 2, 3, and 4, respectively. The binding of native C3 to the peptides was measured at a flow of 30 μl/min; the association and the dissociation phases were 120 s each. Regeneration was achieved by injecting 1- to 2-s pulses of 0.2 M sodium carbonate (pH 9.5).

N-terminal residue and biotransformation studies

To assess whether the increased activity of Ac-compstatin over compstatin was due to the protection of the first amino acid (Ile) against proteolytic cleavage or to the neutralization of the positive charge of the free N terminus of the peptide, we performed the following experiment. Various concentrations of peptides were mixed with 8 μl of NHS, 5 μl of 0.1 M Mg^{2+} EGTA, and 10 μl of Er (10^9 cells/ml), and the final volume was adjusted to 100 μl with GVB. The reaction mixture was incubated at 37°C for 30 min, and the reaction was stopped by addition of 200 μl of GVB with 10 mM EDTA. After centrifugation, the supernatants were mixed with equal volume of 0.1% TFA in H_2O and were centrifuged through 5K cutoff filters. The filtrates containing the free peptides and their bioproducts were analyzed by analytical chromatography on a reversed-phase C-18 column.

Results

Screening of phage-displayed library

We constructed a 13-mer library with the scheme Xaa^1-Cys^2-Val^3-Xaa^4-Gln^5-Asp^6-Trp^7-Gly^8-Xaa^9-Xaa^{10}-Xaa^{11}-Cys^{12}-Xaa^{13} to investigate and optimize the structural elements that contribute to the activity and structural stability of compstatin, besides the β-turn and disulfide bridge-forming amino acids and Val^3 of the hydrophobic cluster. In this study, the constructed library was directly plated on Luria-Bertani plates without amplification so that each plaque would represent a different clone. Individual plaques were then amplified in *E. coli*, and the supernatants were tested for binding to native C3 using ELISA. A total of 800 clones were screened from this library. To ensure the specific binding, only the clones giving absorbance at 405 nm >0.6 were considered positive (Table I). The C3-binding clones show preservation of the hydrophobic character of the linked termini, segment of residues 1–4 and 12–13, and preference for predominantly polar character at the segment of residues 9–11 (Table I). We also sequenced seven randomly selected clones that exhibited no binding to C3 (Table II). The amino acid sequence of these clones shows the presence of proline(s) inside the ring. It is possible that the presence of proline residue results in alteration of the structure of compstatin, which could have an impact on its binding to C3.

Evaluation of the selected clones

Supernatants of the positive clones were plated and the number of plaque forming units in each phage stock was determined. The appropriate dilutions were made, so that each solution would contain 10^8 PFU/μl. The solutions were then examined for their ability to bind C3 using ELISA. The binding curves for each clone (Fig. 1) showed that the phages do not bind to the same extent to C3. As shown, clone 640 bound with the highest potency, whereas clone 8 bound moderately to C3. Although the remaining two clones clearly bound to C3, the potency of their binding was low. This different degree of binding potency could be due to 1) the different affinity of each expressed peptide to C3, 2) the different degree of proteolytic susceptibility of each phage-displayed peptide during the amplification step in *E. coli*, or 3) the heterogeneity of the mixtures. M13 expresses three to five copies of protein III (and consequently of the expressed peptide), and phages with a higher number of copies on their surface will bind tighter to the protein target due to avidity effect.

To examine the above-mentioned possibilities, we chemically synthesized peptides corresponding to the amino acid sequence of the phage-displayed peptides of clones 640, 8, 733, and 774 and of Ac-compstatin (all with acetylated N terminus and C terminus blocked by the NH_2 group). We measured the inhibition of phage-bound compstatin (compstatin-phage) binding against C3 by these five peptides using ELISA (Table III).

As shown in Table III, the ability of the peptides to inhibit the binding of compstatin-phage to C3 differed. These results show that the peptide Ac-I1L/H9W/T13G, which resulted from clone 640, inhibits the compstatin-phage binding to C3 to the same degree as does Ac-compstatin. Interestingly, the peptide that resulted from clone 8 seems to be >23 times less active than compstatin in this experimental setting. This peptide in the direct binding assay (in the form of phage) bound to almost the same extent as did

Table I. *Amino acid sequence of the random insert of C3-binding clones identified through the phage-displayed peptide library screening*

Clone	Amino Acid Sequence[a]
Compstatin	**I**C**V**V**QDWG**HHR**C**T
8	L**C**V**W****QDWG**RHQ**C**F
640	L**C**V**V****QDWG**WHR**C**G
733	S**C**V**F****QDWG**RLA**C**P
774	M**C**V**H****QDWG**GHR**C**F

[a] Bold residues denote amino acids that are fixed in the phage library.

Table II. *Amino acid sequence of the non-C3-binding clones identified through the phage-displayed peptide library screening*

Clone	Amino Acid Sequence[a]
Compstatin	**ICV**V**QDWG**HHR**C**T
12	S**CV**S**QDWG**RD**P**C**S**
18	R**CV**P**QDWG**TP**W**C**P**
50	G**CV**G**QDWG**AP**AC**G
62	D**CVTQDWG**TP**LC**K
120	V**CVIQDWG**QP**SC**G
150	L**CV**P**QDWG**QNG**CW**
171	G**CVAQDWG**P**S**V**C**G

[a] Bold residues denote amino acids that are fixed in the phage library. Prolines are underlined.

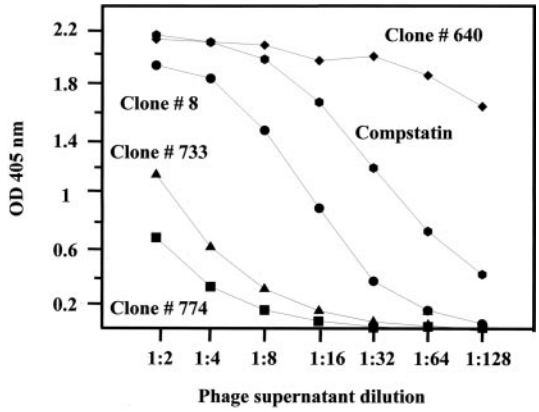

FIGURE 1. Direct binding of phage clones to immobilized C3. Microtiter wells were coated with 500 ng of C3, saturated with 1% milk, washed, and incubated with various dilutions of phage clones. The starting dilution for each phage was 10^8 PFU/μl. Binding of phages was detected by HRP-conjugated anti-M13 Ab.

compstatin (Fig. 1). These data suggest that clone 8 in its multivalent form (phage, where three to five copies of the peptide are expressed) binds with higher affinity to C3 than when in its monovalent form (peptide), which implies that it could have a propensity for oligomerization when copies of this peptide are in close proximity (as is the case when this peptide is expressed on the phage). The pattern of the inhibitory activities of the peptides resulting from clones 733 and 774 is in agreement with the data obtained from their direct binding to C3 (Table III and Fig. 1).

In vitro inhibition of the activation of alternative pathway of complement

The inhibitory activity of the peptides was further examined using the standard hemolytic assay for the inhibition of the activation of the alternative pathway of the complement system. The pattern shown here (Table IV) agrees in general with the pattern of the activities of the synthetic peptides measured during the inhibition of compstatin-phage binding to C3 (Table III). All of the peptides were tested multiple times ($n \geq 7$) and were able to inhibit complement activation. Interestingly, the activity of the peptide Ac-I1L/H9W/T13G (IC_{50} = 2.9) was 1.6 times more active than compstatin (IC_{50} = 4.5). The most significant sequence difference of the peptide Ac-I1L/H9W/T13G from compstatin is the amino acid in position 9 (His^9Trp). Our previous studies have shown that replacement of the same residue by alanine (in the analog Ac-H9A) also resulted in a 1.6-fold increase in activity. The two additional differences, outside the cyclic ring, of the Ac-I1L/H9W/T13G analog compare with Ac-compstatin (Ile^1Leu and Thr^{13}Gly), because Ile is equally hydrophobic to Leu and Thr is more hydrophobic than the neutral Gly. However, a small contribution to activity and possible small compensatory effects may be present due to the replacements at the termini.

NMR studies

We performed homonuclear 2D NMR studies to test the consistency of the structures of Ac-compstatin and acetylated synthetic peptide corresponding to clone 640 (Ac-I1L/H9W/T13G) with the structure of parent peptide compstatin.

Ac-I1L/H9W/T13G compstatin analog

Fig. 2 shows the side chain proton (in δ_1) backbone amide and the aromatic proton (in δ_2) region of the 2D TOCSY spectrum of Ac-I1L/H9W/T13G, where all 13 residues are identified and proton resonances are assigned.

Fig. 3 shows different portions of the 2D NOESY spectrum, which have been used to identify the structure of Ac-I1L/H9W/T13G. A β-turn consists of four residues that provide reversion of the backbone direction, where backbone protons of residues 2–4 show characteristic NOEs of variable intensities depending on spatial proximity. Specifically, strong intensity $H^N(3)$-$H^N(4)$ NOE, medium intensity $H^\alpha(3)$-$H^N(4)$ NOE, and medium-weak intensity $H^\alpha(2)$-$H^N(4)$ NOE are observed for a type I or type II β-turn, where numbers 2–4 denote residues 2–4 of the β-turn. NOEs between residues 2 and 3 discriminate a type I from a type II β-turn. These are strong intensity $H^N(2)$-$H^N(3)$ NOE and medium-weak intensity $H^\alpha(2)$-$H^N(3)$ NOE for a type I β-turn, as opposed to very weak (or absent) intensity $H^N(2)$-$H^N(3)$ NOE and strong intensity $H^\alpha(2)$-$H^N(3)$ NOE for a type II β-turn (23, 24). Because small peptides in solution form ensembles of interconverting conformers, the observed NMR parameters are averaged. In favorable cases, a β-turn conformation forms a significant population that can be observed by NMR. In such cases, it is meaningful to compare the relative intensities of the aforementioned NOEs, where NOEs of the same type suffer similar averaging, rather than absolute intensities.

Fig. 3*A* shows the $H^\alpha(\delta_1)$-$H^N(\delta_2)$ region of the 2D NOESY spectrum of Ac-I1L/H9W/T13G. All sequential connectivities linking $H^\alpha(i)$-$H^N(i)$ and $H^\alpha(i)$-$H^N(i + 1)$ NOEs are observed and marked in the figure. To have a structure consistent with the presence of a β-turn in the same region as in compstatin (Gln^5-Asp^6-Trp^7-Gly^8), a weak intensity for $Asp^6(H^\alpha)$-$Gly^8(H^N)$ should be observed. A cross peak with weak intensity is observed at this position (Fig. 3*A*, arrow), but it cannot be unambiguously assigned to $Asp^6(H^\alpha)$-$Gly^8(H^N)$ NOE because of overlap with the expected $His^{10}(H^\alpha)$-$Arg^{11}(H^N)$ NOE. In addition, NOEs of similar intensity are observed for $Asp^6(H^\alpha)$-$Trp^7(H^N)$ and $Trp^7(H^\alpha)$-$Gly^8(H^N)$ (Fig. 3*A*), which are characteristic of a β-turn but also of extended structures. Fig. 3*B* shows the $H^N(\delta_1)$-$H^N(\delta_2)$ region of the NOESY spectrum, where NOEs of similar intensity are observed for $Asp^6(H^N)$-$Trp^7(H^N)$ and $Trp^7(H^N)$-$Gly^8(H^N)$. Given that the intensities of $Asp^6(H^N)$-$Trp^7(H^N)$ and $Trp^7(H^N)$-$Gly^8(H^N)$ NOEs are similar, we conclude that our data are consistent with the presence of a type I β-turn in the region Gln^5-Asp^6-Trp^7-Gly^8 as in the parent peptide compstatin.

Ac-compstatin

Fig. 4 shows the side chain proton (in δ_1) backbone amide and aromatic proton (in δ_2) region of the 2D TOCSY spectrum of Ac-compstatin, where all 13 residues are identified and proton resonances are assigned. Addition of the acetyl group at the amino-terminal residue makes visible the amide proton resonance of Ile^1

Table III. *Amino acid sequences of synthetic Ac-compstatin and analogs corresponding to the binding clones of Table I and their IC_{50} values for the inhibition of compstatin-phage binding to C3*

Synthetic Peptide	Amino Acid Sequence[a]	IC_{50} (μM)[b]
Ac-compstatin	Ac-ICVVQDWGHHRCT-NH_2	5.6
Peptide 8	Ac-**L**CV**W**QDWG**R**H**Q**C**F**-NH_2	131
Peptide 640 Ac-I1L/H9W/T13G	Ac-**L**CVVQDWG**W**HRC**G**-NH_2	5.4
Peptide 733	Ac-**S**CV**F**QDWG**RLA**C**P**-NH_2	28.8
Peptide 774	Ac-**M**CV**H**QDWG**G**HRC**F**-NH_2	85.2

[a] Underlined and bold amino acids show differences from Ac-compstatin.
[b] ELISA competition binding experiment.

Table IV. *Amino acid sequences and complement inhibitory activities of synthetic compstatin, Ac-compstatin, the analog with His9Ala replacement, analogs corresponding to the binding clones, and analogs with charged side chains at position 1*

Synthetic Peptide	Sequence[a]	IC_{50} (μM)[b]
Compstatin[c]	ICVVQDWGHHRCT-NH_2	12
Ac-compstatin[d]	**Ac**-ICVVQDWGHHRCT-NH_2	4.5
Ac-H9A[e]	**Ac**-ICVVQDWG**A**HRCT-NH_2	2.9
Peptide 8	**Ac**-**L**CV**W**QDWG**R**H**Q**C**F**-NH_2	254
Peptide 640 Ac-I1L/H9W/T13G[f]	**Ac**-**L**CVVQDWG**W**HRC**G**-NH_2	2.9
Peptide 733	**Ac**-**S**CV**F**QDWG**RLA**C**P**-NH_2	24
Peptide 774	**Ac**-**M**CV**H**QDWG**G**HRC**F**-NH_2	87.4
Ac-I1R	**Ac**-**R**CVVQDWGHHRCT-NH_2	8
Ac-I1D	**Ac**-**D**CVVQDWGHHRCT-NH_2	22

[a] Sequence differences that have resulted in altered inhibitory activity increase when compared with the parent peptide compstatin are bold for acetylation and are bold and underlined for specific amino acid replacements.
[b] Inhibition of complement-mediated Er lysis experiment.
[c] Parent peptide compstatin (1, 10).
[d] Second generation parent peptide Ac-compstatin (8).
[e] Previously rationally designed with improved activity compared with parent peptide Ac-compstatin (12).
[f] Designed with the new phage-displayed library described in this work and equally active as the Ac-H9A analog.

(Fig. 4), which was invisible in nonacetylated compstatin (unblocked Ile^1) due to fast exchange with the solvent (10). The TOCSY spectrum is very similar to that of nonacetylated compstatin (10), with the exception of significant shifts of the amide proton resonances of Cys^2 and Val^3 and the α protons of Ile^1 and Cys^2 and smaller shifts of the amide proton resonances of residues Val^4 and Gln^5 (Fig. 4 and Ref. 10). These chemical shift differences are located in the amino-terminal leg of compstatin and reflect a local perturbation introduced by acetylation.

Fig. 5 shows portions of the backbone region of the 2D NOESY spectrum of Ac-compstatin that contain NOE cross peaks that are consistent with the presence of a type I β-turn in the segment Gln^5-Asp^6-Trp^7-Gly^8, as was the case with nonacetylated compstatin (10). Fig. 5*A* shows the $H^{\alpha}(\delta_1)$-$H^{N}(\delta_2)$ region of the 2D NOESY spectrum, where all expected sequential NOE connectivities are drawn. As in the case of nonacetylated compstatin (10), a medium-weak H^{α}-H^{N} NOE between Asp^6 and Gly^8 cannot be unambiguously assigned because of spectral overlap with the strong Trp^7 H^{α}-Gly^8 H^{N} NOE (Fig. 5*A*, arrow). Fig. 5*B* shows the backbone amide proton (in both δ_1 and δ_2) region of the 2D NOESY spectrum of Ac-compstatin, which depicts equal-intensity NOEs between the amides of Asp^6-Trp^7 and Trp^7-Gly^8. These NOEs are characteristic of the presence of a type I β-turn.

Interaction between native C3 and Ac-compstatin or its analogs using the surface plasmon resonance technology

In a previous study, we showed that the nature of the interaction between Ac-compstatin and C3 did not follow the simple 1:1 Langmuir model (8). However, the concentrations of the analyte used were below or near the observed K_D (130 nM). In the present study, we repeated surface plasmon resonance measurements using analyte concentrations lower and higher than the previously observed K_D (62.5–2000 nM). In addition, we examined the nature of the interaction between the Ac-I1L/H9W/T13G and Ac-H9A with C3.

We synthesized analogs of Ac-compstatin, Ac-I1L/H9W/T13G, and Ac-H9A containing an extra spacer sequence of 14 amino acids at the C terminus end. This sequence, Ala-Gly-His-Met-Ala-Asn-Leu-Thr-Ser-His-Ala-Ser-Ala-Lys, was derived from the original phage-clone of compstatin (1). We decided to add the extra spacer sequence to increase the accessibility of native C3 to the 13 amino acids constituting Ac-compstatin, Ac-H9A, and Ac-I1L/H9W/T13G. The peptides were biotinylated at the C terminus and were immobilized on streptavidin chips. In a previous study we showed that only when the peptide is immobilized through the C terminus is it able to bind native C3 (8), a fact that underlines the importance of the accessibility of the N terminus region of compstatin and its analogs for their binding to C3. In addition, the biotinylated 27-mer peptide (ICVVQDWGHHRCTAGHMANLT SHASAK-biotin) exhibits the same activity as compstatin in the presence or absence of avidin (data not shown). The C3 used for this analysis was freshly prepared and was >90% pure. To ensure the removal of $C3(H_2O)$ from the preparation, we further purified the analyte sample using a mono-S column (Pharmacia). In this way, we were able to preserve a homogeneous surface along with a homogeneous analyte sample, thus minimizing any artifacts that would interfere with our study. The homogeneity of the surface and the analyte sample is critical when Biacore analysis is used, given that heterogeneity can give false kinetic profiles. The profiles of the surface plasmon resonance measurements for the binding of Ac-compstatin and its analogs to native C3, shown in Fig. 6, were reproducible in Biacore-X and Biacore-3000 in multiple experiments. None of the sensograms fit the simple 1:1 Langmuir model when analyzed with BIAevaluation 3.0 software (25). We examined the data of the association phase by linear transformation analysis (8).

As shown in Fig. 7, none of the linear transformation plots yielded a straight line, suggesting that all of these interactions follow more complex models. In addition, a closer look at the profiles of the linear plots for Ac-compstatin-C3 binding showed that in low concentrations of analyte (62.5–250 nM) there was clearly an interaction that is composed of more than one step (Fig. 7*A*). However, in higher concentrations (500–2000 nM) it was not as profound (Fig. 7*B*). These kinds of plots could be characteristic of bivalent binding (i.e., following the traditional $A + 2B \leftrightarrow AB_2$ mechanism or there could exist two sites of interaction in either of the reactants). This is different from an earlier indication that binding of compstatin is biphasic (8). Given the current limitations of surface plasmon resonance methods, it is not possible to provide a precise binding mechanism. However, our current and previous data clearly show that the interaction between Ac-compstatin and C3 is more complex than a 1:1 relation.

Finally, this pattern was not observed for the interaction between Ac-H9A or Ac-I1L/H9W/T13G and C3 (Fig. 7, *C* and *D*). For these peptides, the linear transformation plots were similar in all of the concentrations of C3 used. Despite this, the association data of the sensogram for Ac-H9A or Ac-I1L/H9W/T13G (Fig. 6, *B* and *C*) did not fit the 1:1 Langmuir model when analyzed with

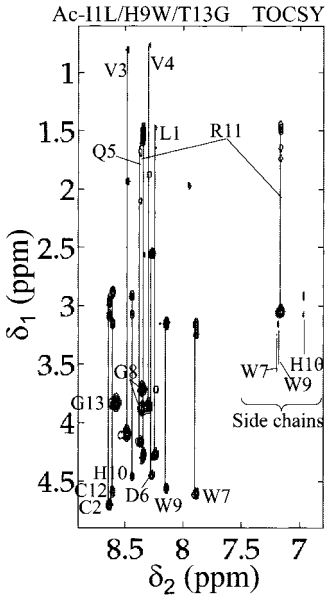

FIGURE 2. Portion of the 2D TOCSY spectrum of Ac-I1L/H9W/T13G that shows the identification of all 13 residues.

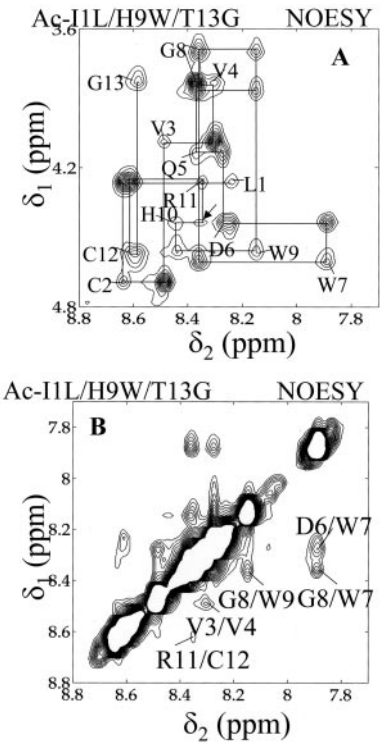

FIGURE 3. *A*, The $H^{\alpha}(\delta_1)$-$H^{N}(\delta_2)$ region of the 2D NOESY spectrum of Ac-I1L/H9W/T13G that shows intraresidue and (i, i + 1) sequential NOE connectivities. *B*, The $H^{N}(\delta_1)$-$H^{N}(\delta_2)$ region of the 2D NOESY spectrum of Ac-I1L/H9W/T13G that shows (i, i + 1) sequential NOE connectivities.

BIAevaluation 3.0 software. This suggests that both peptides interact with C3 with a more complex mechanism that differs from the one that characterizes the Ac-compstatin-C3 interaction.

Contribution of the N-terminal amino acid to the activity of compstatin

In previous studies it was shown that acetylation of the N-terminal amino acid of compstatin resulted in an approximately 3-fold increase in its activity, as shown by inhibition of the complement pathway activation in vitro (8, 9). We then hypothesized that this was due to the protection of the N-terminal amino acid against proteolytic cleavage by serum proteases (8). This was supported by our data showing that the N terminus of the nonacetylated peptide was proteolytically cleaved when incubated in whole human serum, whereas the acetylated peptide was not cleaved. However, the conditions under which the stability of the peptides was examined were different from the ones used to evaluate their activities. The stability of the peptides was examined in whole serum over a long period of time, whereas their activity was assessed using the classic experiment of inhibition of complement activation in which diluted serum is used and the incubation lasts for 25 min.

In the present study, different concentrations of compstatin with or without N-terminal acetylation were incubated with diluted serum and Er in the presence of Mg^{2+}EGTA (conditions under which the alternative pathway is conducted). The mixtures after a 25-min incubation at 37°C were spun through 5K filters, and the bioproducts of the peptides were analyzed using reversed-phase column chromatography. The area of the peaks of the uncleaved peptide was calculated and is shown in Fig. 8; the quantities of the uncleaved compstatin and its acetylated analog, after the end of the incubation, were comparable. We assigned as 100% the amount of Ac-compstatin that remained uncleaved after the lysis experiment. The amount of compstatin that remained stable throughout the lysis experiment was 95% of that of its acetylated form. However, this small difference in the stability cannot account for the approximately 3-fold difference in their activity. This observation is indicative that the increase of the activity was not due to the protection of the N terminus against proteolytic cleavage. In a follow-up structural study of several compstatin analogs, we proposed that acetylation at the N terminus resulted in removal of the positive charge of the amide of amino acid 1. This charge elimination resulted in enhancement of the hydrophobic clustering at the termini, which is necessary for binding to C3 (12).

In our attempt to further test the charge elimination hypothesis, we performed two additional control experiments that reintroduced charge. We prepared acetylated compstatin analogs with side chain, instead of backbone, charge at position 1. We examined the activity of these analogs by measuring the inhibition of the activation of the alternative pathway of the complement system. In one of them, Ac-I1R, in which Ile^1 was replaced by positively charged Arg that imitates the positive charge of the amino terminus of the unblocked peptide, the inhibitory activity was reduced by 2-fold. Because this analog is acetylated, the decrease in activity is attributed to the positive charge of the Arg side chain that disrupts the hydrophobic cluster at the termini. This is in agreement with the approximately 3-fold increase of activity in the opposite design, where the N-terminal amino acid Ile was neutralized by acetylation (Table IV). The small activity difference in the two designs may reflect the spatial position of the positive charge at the N terminus or the side chain of Arg. In the other analog, Ac-I1D, in which the negatively charged Asp replaced Ile^1, the inhibitory activity was further reduced by 5-fold (Table IV). Because this analog is acetylated, the additional decrease in activity is attributed to the presence of the negative charge of the Asp side chain, which is less favored than the positive charge and much less favored than a hydrophobic residue. These data are consistent with our current hypothesis that elimination of charge and not elimination of cleavage is the cause of the higher activity of acetylated compstatin compared with nonacetylated compstatin (12).

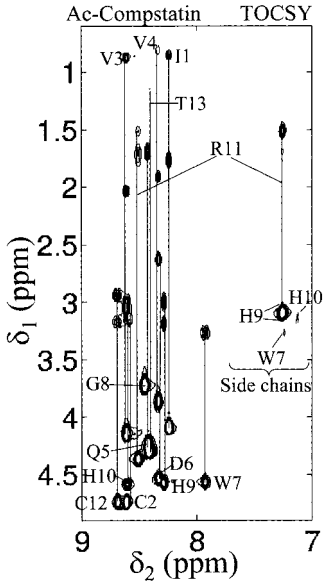

FIGURE 4. Portion of the 2D TOCSY spectrum of Ac-I1L/H9W/T13G that shows the identification of all 13 residues.

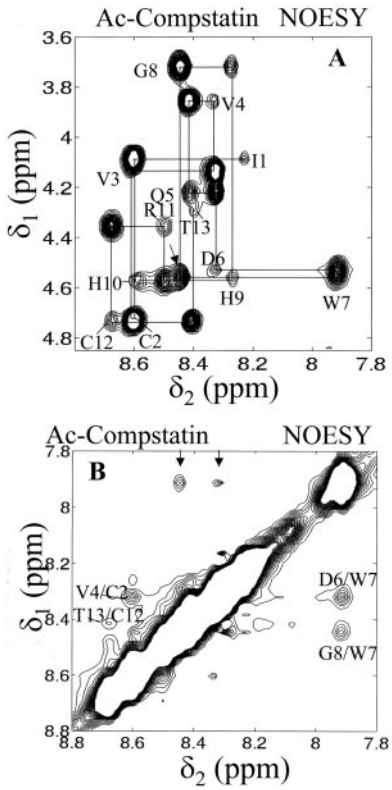

FIGURE 5. *A*, The $H^{\alpha}(\delta_1)$-$H^{N}(\delta_2)$ region of the 2D NOESY spectrum of Ac-compstatin that shows intraresidue and (i, i + 1) sequential NOE connectivities. *B*, The $H^{N}(\delta_1)$-$H^{N}(\delta_2)$ region of the 2D NOESY spectrum of Ac-compstatin that shows (i, i + 1) sequential NOE connectivities. The arrows show regions of negative t_1 ridges that attenuate the intensities of the overlapping cross peaks.

Discussion

The complement system is the first line of defense against foreign pathogens. However, excessive activation and failure in the intrinsic regulation of the complement system during surgical procedures or pathological situations results in tissue injury, which underlines the importance of development of effective complement inhibitors. Currently none is available in the clinic. Compstatin is a 13-mer peptide discovered in our laboratory that inhibits complement activation in vitro (1) and in vivo (4) through binding to the central component of the system, C3. Compstatin's proven efficacy and its small size are incontrovertible advantages that render it one of the most promising inhibitors of the activation of the complement system.

Compstatin forms a type I β-turn in the region Gln^5-Asp^6-Trp^7-Gly^8 (10). In addition, compstatin possesses a hydrophobic cluster at the opposite side of the β-turn involving residues around the linked termini Ile^1-Cys^2-Val^3-Val^4-Cys^{12}-Thr^{13}. We have previously proposed that the four residues of the β-turn and the disulfide bridge between Cys^2-Cys^{12} are necessary for both structural stability and inhibitory activity of compstatin. Indeed, the β-turn provides change in the direction of the structure and sufficient separation of the two sides of compstatin, whereas the disulfide bridge prevents them for drifting apart. It is known that β-turns provide structural stability and facilitate the molecular interaction through the clustering of the side chains. We have also proposed that three of six residues of the hydrophobic cluster (Cys^2-Val^3-Cys^{12} of Ile^1-Cys^2-Val^3-Val^4-Cys^{12}-Thr^{13}) are essential for inhibitory activity of compstatin. This current hypothesis is based on activity and structural studies of a large number of single, double, and triple replacement analogs (8, 10, 12). The present study was undertaken with the aim to further understand the structure-function relation of compstatin and to design a better (more active) compstatin analog, using as a basis the wealth of our previous structural and activity data. To evaluate the contribution of the structural elements other than the β-turn and hydrophobic cluster forming amino acids to compstatin's activity, we constructed a phage-display random peptide library with the scheme Xaa^1-Cys^2-Val^3-Xaa^4-Gln^5-Asp^6-Trp^7-Gly^8-Xaa^9-Xaa^{10}-Xaa^{11}-Cys^{12}-Xaa^{13}. The screening of the library produced four positive clones (Table I). These peptides share the overall sequence characteristics of compstatin and previously determined active analogs of compstatin. Specifically, the hydrophobic character of the termini and the predominantly polar character of the β-turn containing segment 5–11 are preserved. The hydrophobic cluster of Ac-compstatin consists of the set of amino acids Ile, Val, Cys, and Thr, and the corresponding region of the most active phage analog, Ac-I1L/H9W/T13G, consists of Leu, Val, Cys, and Gly. Given that Thr is partially hydrophobic (because of the existence of a methyl group) and partially polar (because of the existence of a hydroxyl group) and Gly is a neutral group, the composition of the hydrophobic cluster may be only slightly different in the two peptides. The polar region of Ac-compstatin and Ac-I1L/H9W/T13G consists of the same set of amino acids (Gln, Asp, Trp, Gly, His, and Arg), with the difference that His occurs twice in Ac-compstatin, whereas Trp occurs twice in Ac-I1L/H9W/T13G.

We also sequenced seven negative clones (Table II). All of the negative clones preferentially have a Pro between the Cys^2 and Cys^{12}. Because these were inactive clones, we did not perform NMR studies to determine their structure. The fact that all of the peptides produced by the screening of the phage library that contained the fixed amino acids without the presence of Pro inside the ring bound to C3 suggests that Pro may be destabilizing the structure of these peptides. Furthermore, our previous data suggest that the fixed components of our library (Val^3; the disulfide bridge $Cys^{2,12}$; and the β-turn forming amino acids Gln^5, Asp^6, Trp^7, and Gly^8) are the vital components of compstatin for its binding to C3. Therefore, we believe that if these amino acids are fixed, only major disruptions of its structure (such as the presence of proline)

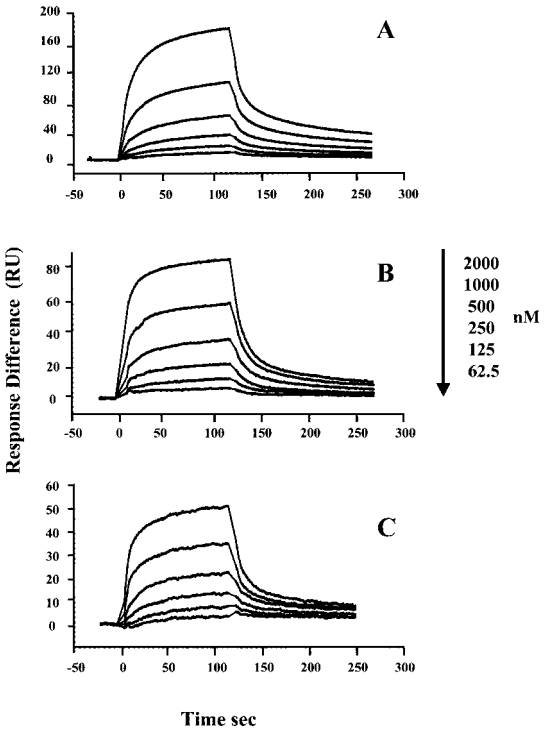

FIGURE 6. Sensograms for the interaction with C3 of immobilized biotinylated Ac-compstatin (*A*), Ac-H9A (*B*), and Ac-I1L/H9W/T13G (*C*). The concentrations of the analyte used are indicated at *right.*

could negatively influence the binding capacity of the peptide to C3.

Indeed, in a previous study of ours, an analog that included a Pro instead of an Asp at position 6, in addition to Gln^5Gly and Trp^7Phe substitutions, was both inactive and structurally distorted compared with compstatin (12). However, there is the possibility that there are other clones that do not contain proline and exhibit no binding to C3. The experimental complexity of phage libraries does not always correspond to the theoretical number of expected peptides, and as a result certain amino acids (proline in our case) are favored over others due to biological selection during the phage formation. This could explain why the presence of proline is preferential in the nonbinding clones.

It is clear that the physicochemical nature of the nonfixed amino acids (positions 1, 4, 9–11, and 13) has an effect on the activity of the peptide. As shown in Table I, all of the peptides that were selected from the screening of the phage library contain the β-turn -forming amino acids and hydrophobic amino acids at the termini, but their activities vary (Table IV). This can only be attributed to the six remaining amino acids (positions 1, 4, 9–11, and 13) and their effects on structure and binding to C3.

The peptide that is derived from the sequence of clone 640, Ac-I1L/H9W/T13G (Tables I and IV), was the only peptide produced by the phage library screening that was more active than compstatin (by 4-fold) and Ac-compstatin (by 1.6-fold) during in vitro inhibition of the activation of an alternative pathway of the complement system. The most evident difference between the Ac-I1L/H9W/T13G and Ac-compstatin is the presence of Trp in position 9 instead of His. The importance of the amino acid at position 9 has also been demonstrated previously, when substitution of His^9 by Ala (Ac-H9A) resulted in an increase in inhibitory activity by 1.6-fold (12). The substitutions in positions 1 and 13 in the Ac-I1L/H9W/T13G could also play a minor role in modulating the activity of this analog. It is possible that replacing the dual character amino acid Thr with Gly slightly affects the hydrophobicity of the cluster.

The consistency of the structures of Ac-compstatin and Ac-I1L/H9W/T13G with the structure of compstatin was examined using NMR analysis. The NMR spectra of Ac-compstatin have been presented here for the first time. The spectra show that acetylation and replacement of His^9 with Trp did not have an effect on the structural stability of the type I β-turn, which remained intact spanning residues Gln^5-Asp^6-Trp^7-Gly^8 as in parent peptide compstatin. Some structural changes at the termini because of acetylation and Ile^1Leu and Thr^{13}Gly replacements may be present.

Comparison of the Ac-I1L/H9W/T13G and Ac-H9A analogs that have the same inhibitory activity (Table IV), suggests that small compensatory effects in inhibitory activity, due to the differences of Ile/Leu at position 1, Trp/Ala at position 9, and Thr/Gly at position 13, are present. It is not clear why the bulky Trp at position 9 compares about equally in terms of activity with the small Ala. However, there may be some similarity. Ala has hydrophobic character (because of the methyl group) and polar character, in that it can be found at the interior and the surface of proteins (because of lack of methylene or an additional methyl group). Trp is partially polar (because of the indole amide group) and partially hydrophobic (because of the aromatic ring).

Our current data suggest that the side chains of some of the fixed amino acids play the major role in the interaction of compstatin with C3. A key residue of the β-turn is Trp^7. It is noteworthy that our previous study showed that replacement of Tpr7 by Phe resulted in a complete loss of the activity (12). Nevertheless, this analog had preserved the structure of the parent peptide.

We further compared compstatin, Ac-I1L/H9W/T13G, and Ac-H9A for binding to C3 using Biacore technology. This part of the study shows that Ac-compstatin and the analog peptides interact with C3 after a more complex mechanism than one-to-one interaction. Interestingly, as shown by the linear transformation plots (dR/dt vs R), when low concentrations of C3 (62.5–250 nM) were used, the interaction between Ac-compstatin and C3 followed a mechanism that consists of more than one component (Fig. 7*A*). Specifically, the dR/dt vs plot is not linear (which would imply 1:1 interaction), rather it is composed of at least two components, thus suggesting that a more than one-step interaction takes place. This is in agreement with previous studies of our laboratory in which we showed that Ac-compstatin interacts with C3 in a manner that is more complex than one-to-one binding (8). In the present study, in which we used high concentrations of analyte (500–2000 nM), we could not observe the same profiles (Fig. 7*B*). This pattern was not observed for the interaction of Ac-H9A or Ac-I1L/H9W/T13G with C3 when the same range of concentration was used. The linear transformation plots for these peptides were very similar (Fig. 7, *C* and *D*) at all concentrations used. Given that the analyte was the same in all cases (native C3), we concluded that the difference in the kinetic profiles of Ac-compstatin and Ac-H9A or Ac-I1L/H9W/T13G binding to C3 is due to the differential C3-binding properties of the peptides, because of differences in their amino acid composition.

It has been shown that the peptide Ac-H9A has a more flexible structure outside the β-turn when compared with that of Ac-compstatin (12). The different profiles of the linear transformation plots between Ac-compstatin and Ac-H9A could be attributed to the variability of the structure of the latter peptide. Nevertheless, the Ac-I1L/H9W/T13G analog, despite the fact that it has similar kinetic profiles with Ac-H9A, has a structure that probably lacks flexibility (Figs. 2 and 3) and is more similar to the structure of compstatin. We have determined previously that Trp^7 is an indispensable residue for activity (12). The presence of a second Trp at

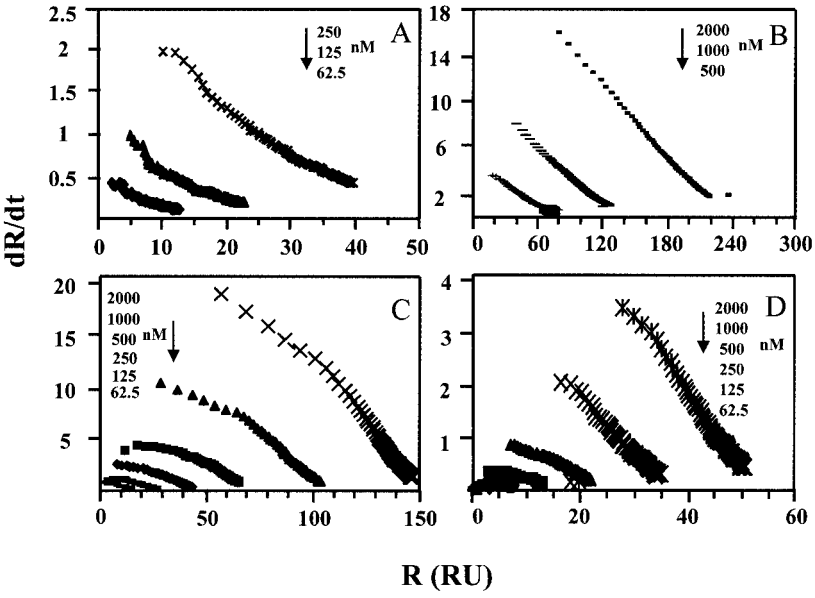

FIGURE 7. Linear transformation of the association phase data for the interaction of Ac-compstatin with low (*A*) and high concentration (*B*) with native C3. Linear transformation of the association phase data for the interaction of Ac-H9A (*C*) and Ac-I1L/H9W/T13G (*D*) with native C3.

position 9 in the Ac-I1L/H9W/T13G analog may be indicative of the importance of π-orbital stacking from the two Trp rings for binding to C3. It is not unlikely that the Trp residues contribute to binding via some type of dipole-dipole interactions with the added possibility of hydrogen bond formation from their indole amide protons. The Trp ring packing may have a compensatory effect for the loss of flexibility outside the β-turn when comparing the Ac-I1L/H9W/T13G to the Ac-H9A analog, given that the two analogs have similar activities. The structural data in combination with the kinetic data suggest that the difference in the binding profiles is owed to gain or loss of structural flexibility combined with the presence of a single or a pair of Trp residues.

As mentioned above, a critical element for the interaction between compstatin and C3 is the hydrophobicity of the termini. In previous studies it was shown that acetylation of the N terminus resulted in an approximately 3-fold increase of the activity (8, 9). We had then hypothesized that this increase was due to the protection of the N terminus by proteolytic cleavage (8). In a later study, we proposed using structural modeling that the increase of the activity was due to the neutralization through acetylation of the positive charge of the N terminus (12). The present study shows that this is actually the case. Incubation of the acetylated and non-acetylated form of compstatin in diluted human serum, and in the conditions under which the alternative pathway is conducted, showed that the quantities of the uncleaved peptides at the end of the experiment were almost equal (5% difference; Fig. 8). Consequently, the observed increased activity of the *N*-acetylated analog of compstatin is not due to its higher stability in human serum, but rather to the neutralization of the N-terminal charge and its direct effect on its interaction with C3.

We further tested the argument that elimination of the N-terminal charge by acetylation resulted in enhancement of the hydrophobic cluster, which in turn resulted in enhancement of binding to C3 and enhancement of complement inhibitory activity. We replaced the N terminus by acetylated charged amino acids, Arg and Asp, which introduced the charge at the side chain instead of the backbone. Both replacements resulted in a decrease of the activity. In particular, the decrease in activity due to the Ile^1Arg replacement (introduction of positive charge) was approximately 2-fold, which compares well with the approximately 3-fold increase of activity in the opposite experiment of introduction of acetylation (removal of N-terminal amide positive charge). Introduction of negative charge with the Ile^1Asp replacement resulted in a more radical approximately 5-fold decrease in activity.

In conclusion, we have shown how a combination of rational design based on structure-activity relations and experimental combinatorial design based on the construction of a phase-displayed peptide library have aided the further understanding of the structure-function relations of compstatin and the identification of a new generation of active compstatin analogs. One of these new analogs, the Ac-I1L/H9W/T13G, is more active than its parent peptides compstatin and Ac-compstatin. It should be noted that compstatin 1) was initially identified using a phage-displayed peptide library, 2) was subsequently optimized for activity using amino acid deletions, insertions, and replacements, 3) after the three-dimensional structure was determined, was further optimized using structural modeling, and 4) based on the overall knowledge of steps 1–3, had further optimization performed using a new phage-displayed library. We performed structure-binding correlations to gain insight into the binding mechanism of the new analog. The structure of the new analog Ac-I1L/H9W/T13G was compared with the structures of Ac-compstatin, compstatin, and the equally active analog AcH9A using NMR and was found to be very similar. The binding to C3 of Ac-I1L/H9W/T13G and Ac-H9A was examined using surface plasmon resonance. This study suggested similarity in binding mechanism between Ac-I1L/H9W/T13G and Ac-H9A, but differences in the binding mechanism when compared with Ac-compstatin. Our binding studies in combination with our earlier structure-activity data (12) suggest that Trp^7 is an essential residue for binding and activity. Introduction of a second Trp in the vicinity, Trp^9, results in stronger binding with altered mechanism and higher activity. Participation of Trp^7 and Trp^9 in binding via dipole-dipole interaction mechanism involving stacked Trp rings is possible, with the added possibility of hydrogen bond formation. Flexibility outside the β-turn possibly compensates the Trp pair stacking with end-result similar binding and activity for the analogs Ac-H9A and Ac-I1L/H9W/T13G. Finally, the significance of the hydrophobic cluster at the linked termini of compstatin was scrutinized by disrupting the hydrophobicity with the introduction of side chain charges at the N terminus. Lack of charge at termini is essential for improved binding to C3 and complement inhibition. Overall, our data are in agreement with our

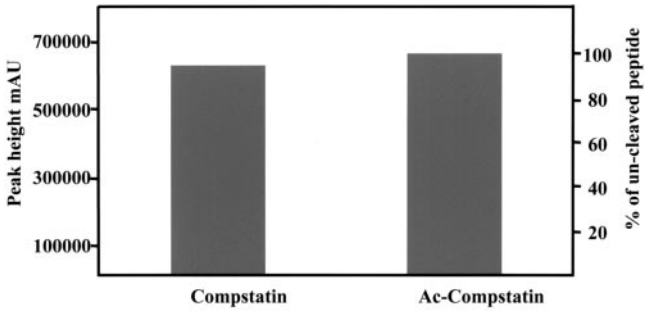

FIGURE 8. In vitro biotransformation of compstatin and Ac-compstatin. The bar graphs correspond with the height of reversed-phase column chromatography peaks of compstatin and Ac-compstatin after being incubated with diluted serum, Er, and Mg^{2+} EGTA (conditions used for the alternative pathway lysis) for 25 min and spun through a 5K filter. The height of Ac-compstatin peak was assigned at 100% and the area of compstatin was accordingly normalized. These values correspond to uncleaved peptides (see *Materials and Methods*).

previous working hypothesis that the structure of compstatin is essential for activity, with the key elements being the β-turn, the hydrophobic cluster, and the presence of Trp^7 (12). The present findings, along with the previous data, are expected to facilitate the design of other peptides or nonpeptidic analogs of compstatin with improved binding properties and activity.

References

1. Sahu, A., B. K. Kay, and J. D. Lambris. 1996. Inhibition of human complement by a C3-binding peptide isolated from a phage displayed random peptide library. *J. Immunol. 157:884.*
2. Fiane, A. E., T. E. Mollnes, V. Videm, T. Hovig, K. Hogasen, O. J. Mellbye, L. Spruce, W. T. Moore, A. Sahu, and J. D. Lambris. 1999. Compstatin, a peptide inhibitor of C3, prolongs survival of ex vivo perfused pig xenografts. *Xenotransplantation 6:52.*
3. Nilsson, B., R. Larsson, J. Hong, G. Elgue, K. N. Ekdahl, A. Sahu, and J. D. Lambris. 1998. Compstatin inhibits complement and cellular activation in whole blood in two models of extracorporeal circulation. *Blood 92:1661.*
4. Soulika, A. M., M. M. Khan, T. Hattori, F. W. Bowen, B. A. Richardson, C. E. Hack, A. Sahu, L. H. Edmunds, Jr., and J. D. Lambris. 2000. Inhibition of heparin/protamine complex-induced complement activation by Compstatin in baboons. *Clin. Immunol. 96:212.*
5. Sahu, A., D. Morikis, and J. D. Lambris. 2000. Complement inhibitors targeting C3, C4, and C5. In *Therapeutic Interventions in the Complement System*. J. D. Lambris and V. M. Holers, eds. Humana Press, Totowa, NJ, p. 75.
6. Sahu, A., and J. D. Lambris. 2000. Complement inhibitors: a resurgent concept in anti-inflammatory therapeutics. *Immunopharmacology 49:133.*
7. Morikis, D., and J. D. Lambris. 2002. Structural aspects and design of low-molecular-mass complement inhibitors. *Biochem. Soc. Trans. 30:1026.*
8. Sahu, A., A. M. Soulika, D. Morikis, L. Spruce, W. T. Moore, and J. D. Lambris. 2000. Binding kinetics, structure-activity relationship, and biotransformation of the complement inhibitor compstatin. *J. Immunol. 165:2491.*
9. Furlong, S. T., A. S. Dutta, M. M. Coath, J. J. Gormley, S. J. Hubbs, D. Lloyd, R. C. Mauger, A. M. Strimpler, M. A. Sylvester, C. W. Scott, and P. D. Edwards. 2000. C3 activation is inhibited by analogs of compstatin but not by serine protease inhibitors or peptidyl α-ketoheterocycles. *Immunopharmacology 48:199.*
10. Morikis, D., N. Assa-Munt, A. Sahu, and J. D. Lambris. 1998. Solution structure of compstatin, a potent complement inhibitor. *Protein Sci. 7:619.*
11. Klepeis, J. L., C. A. Floudas, D. Morikis, and J. D. Lambris. 1999. Predicting peptide structures using NMR data and deterministic global optimization. *J. Comput. Chem. 20:1344.*
12. Morikis, D., M. Roy, A. Sahu, A. Troganis, P. A. Jennings, G. C. Tsokos, and J. D. Lambris. 2002. The structural basis of compstatin activity examined by structure-function-based design of peptide analogs and NMR. *J. Biol. Chem. 277:14942.*
13. Hammer, C. H., G. H. Wirtz, L. Renfer, H. D. Gresham, and B. F. Tack. 1981. Large scale isolation of functionally active components of the human complement system. *J. Biol. Chem. 256:3995.*
14. Pangburn, M. K. 1987. A fluorimetric assay for native C3: the hemolytically active form of the third component of human complement. *J. Immunol. Methods 102:7.*
15. Kay, B. K., N. B. Adey, Y.-S. He, J. P. Manfredi, A. H. Mataragnon, and D. M. Fowlkes. 1993. An M13 phage library displaying random 38-amino acid peptides as a source of novel sequences with affinity to select targets. *Gene 128:59.*
16. Sparks, A. B., N. B. Adey, S. Cwirla, and B. K. Kay. 1996. Construction of random peptide libraries in bacteriophage M13. In *Phage Display of Peptides and Proteins: A Laboratory Manual*. B. K. Kay, J. Winter, and J. McCafferty, eds. Academic Press, San Diego, p. 227.
17. Moore, W. T. 1997. Laser desorption mass spectrometry. *Methods Enzymol. 289: 520.*
18. Angeletti, R. H., L. Bibbs, L. F. Bonewald, G. B. Fields, J. S. McMurray, W. T. Moore, and J. T. Stults. 1996. Formation of disulfide bond in an octreotide-like peptide: a multicenter study. In *Techniques in Protein Chemistry*, Vol. VII. D. R. Marshak, ed. Academic Press, San Diego, p. 261.
19. Sahu, A., and M. K. Pangburn. 1996. Investigation of mechanism-based inhibitors of complement targeting the activated thioester of human C3. *Biochem. Pharmacol. 51:797.*
20. Ernst, R. R., G. Bodenhausen, and A. Wokaun. 1990. *Principles of Nuclear Magnetic Resonance in One and Two Dimension*. Oxford University Press, Oxford, U.K.
21. Piotto, M., V. Saudek, and V. Sklenar. 1992. Gradient-tailored excitation for single-quantum NMR-spectroscopy of aqueous solutions. *J. Biomol. NMR 2:661.*
22. Marion, D., M. Ikura, and A. Bax. 1989. Improved solvent suppression in one-dimensional and two-dimensional NMR-spectra by convolution of time-domain data. *J. Magn. Reson. 84:425.*
23. Wüthrich, K. 1986. *NMR of Proteins and Nucleic Acids*. John Wiley & Sons, New York.
24. Dyson, H. J., M. Rance, R. A. Houghten, P. E. Wright, and R. A. Lerner. 1988. Folding of immunogenic peptide-fragments of proteins in water solution. II. The nascent helix. *J. Mol. Biol. 201:201.*
25. Biacore. *BIAevaluation version 3 Software Handbook*. Biacore.